Atomic-scale friction modulated by a buried interface: Combined atomic and friction force microscopy experiments

S. Maier,[1,*] E. Gnecco,[1] A. Baratoff,[1] R. Bennewitz,[2] and E. Meyer[1]
[1]*Department of Physics and Astronomy, University of Basel, Basel 4056, Switzerland*
[2]*Department of Physics, McGill University, Montreal, Quebec H3A 2T8, Canada*
(Received 28 June 2007; revised manuscript received 23 June 2008; published 31 July 2008)

Combined atomic and friction force microscopy reveals a significant modulation of atomic-scale friction related to the small periodic rumpling induced at the interface between heteroepitaxial films of KBr on NaCl(100). Transitions from dissipative atomic-scale stick slip to smooth sliding with ultralow friction are observed within the 6×6 surface unit cell of the underlying superstructure. Scanning across atomic-scale defects confirms the high-resolution capabilities of friction force microscopy close to the ultralow friction state. Strong variations of the tip-surface interaction energy across the superstructure demonstrate that subsurface chemical and size inhomogeneities dramatically change the frictional properties of the surface probed by the microscope tip.

DOI: 10.1103/PhysRevB.78.045432 PACS number(s): 68.35.Af, 46.55.+d, 68.37.Ps, 68.55.−a

I. INTRODUCTION

The understanding and control of frictional properties on the atomic scale have made tremendous progress since the dawn of friction force microscopy[1] and are of crucial importance, especially in device applications such as microelectromechanical systems (MEMS) and nanoelectromechanical systems (NEMS). One ubiquitous observation in the motion of a nanoscale asperity, i.e., the tip of an atomic force microscope (AFM), across an atomically flat surface is the atomic stick-slip process, where the lateral force grows almost linearly, then suddenly changes at specific locations which reflect the periodicity of the underlying surface lattice. At each force discontinuity, the tip jumps from one surface lattice position to an adjacent one. The characteristics and even the occurrence of stick-slip motion can be tuned by several parameters, such as the normal load applied on the tip,[2,3] the relative orientation of the tip,[4] the scan velocity,[5,6] the temperature,[6–8] or even electromechanical excitation of the contact region.[9] In order to develop new ways of controlling friction, it is crucial to understand how friction depends on the atomic structure of the contacting surfaces. For instance, Park *et al.*[10] found a strong friction anisotropy on the surface of a quasicrystal between the periodic and aperiodic crystal directions. However, most atomic-scale studies based on friction force microscopy have so far been limited to perfectly ordered crystal terraces and in some cases to step edges between them.

In this paper, we investigate the influence of periodic long-range order induced by heteroepitaxial growth of chemically similar materials on atomic friction. Ultrathin films of KBr deposited on NaCl(100) surfaces form a square superstructure with a periodicity of 3.9 nm, equal to six lattice spacings of KBr and seven lattice spacings of NaCl, as revealed by helium atom diffraction,[11] investigated in detail by atomistic simulations,[12] and recently confirmed by noncontact atomic force microscopy.[13] The surface of such films exhibits a small rumpling of the order of 0.1 Å.[12] We present images of the film surface in contact mode which clearly show the KBr lattice and the superstructure, as well as defect-induced atomic-scale distortions, and also interpret the observed load-dependent lateral force traces.

This study shows that a buried interface, which leads to a tiny long-range rumpling at the sample surface, is not observable at low loads but causes large variations of frictional forces at increased loads. Therefore, we conclude that atomic friction depends not only on the surface composition but is also influenced by the presence of interfaces at nanometer depth. The underlying mechanism is attributed to the interaction between elastic strains caused by the sharp probing tip and by atomic-scale mismatch at the interface. Similar effects may occur in the case of a workpiece with nanometer-scale asperities moving parallel to a nominally very smooth ultrathin coating on a substrate with asperities of similar size.

II. EXPERIMENTAL SETUP

Single crystals of NaCl were cleaved in ultrahigh vacuum (UHV) and heated at 150 °C to remove charges produced in the cleavage process. Films were grown *in situ* by evaporating KBr from a Knudsen cell at a rate of 0.1 Å/min on the clean substrate at room temperature. Details about the morphology of the films obtained under different evaporation conditions are described elsewhere.[13] The present measurements were performed on top of nearly perfect two-layer thick KBr islands with a home-built atomic force microscope equipped with a four quadrant optical deflection detector operated in UHV at room temperature.[14] Rectangular silicon cantilevers with spring constants of $k_N=0.05$ N/m for normal bending and $k_T=39.1$ N/m for torsion were used. The normal and lateral forces acting on the tip were calibrated according to the procedure described in Ref. 15. All normal forces are defined with respect to the unbent cantilever, so that negative forces indicate bending of the cantilever toward the sample, owing to partially compensated net attractive forces.

III. RESULTS

A. High-resolution capability of friction force microscopy

Figure 1 shows images of the surface topography (a) and of the lateral force (b) along the forward scan direction si-

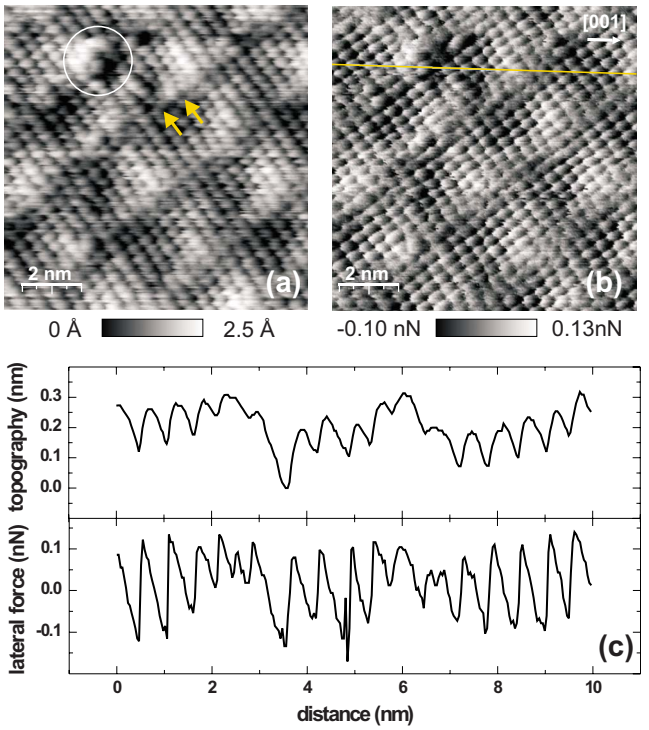

FIG. 1. (Color online) Simultaneously recorded images of (a) the surface topography and of (b) the lateral force at a normal force of −0.01 nN on a KBr double layer deposited on NaCl(100). They reveal the underlying superstructure, as well as atomic-scale modifications (indicated by the circle and arrows) induced by an unidentified defect at the same locations in both images. (c) Topography and lateral force traces across the unidentified defect along the yellow line in (b).

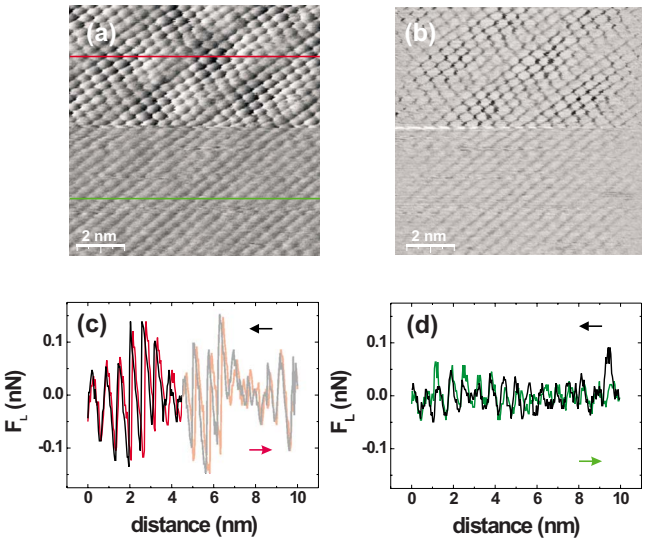

FIG. 2. (Color online) Constant height lateral force image of (a) a KBr double layer on NaCl(100) and [(c) and (d)] corresponding forward and backward traces along the lines indicated in (a). (b) Difference between lateral forces recorded in successive forward and backward scans. The average normal force was reduced from −0.01 to −0.32 nN in the lower half of the image.

multaneously measured on top of a KBr double layer island on NaCl(100) in soft contact mode. The lateral force exhibits sharper variations than the topography, also evident in the corresponding traces (c). The vertical jumps in the lateral force nearly coincide with smoother rises and broader, more symmetric maxima in the vertical position of the cantilever holder because the height control feedback cannot faithfully follow the rapid variations of the normal force which accompany each slip. Together with the atomic lattice, a fairly regular superstructure with a periodicity of six KBr unit cells is clearly visible in the right bottom half of both images. Significant deviations from both periodicities are found around the asymmetric feature inside the circle in Fig. 1(a). Very similar distortions are observed in Fig. 1(b) and in the traces of Fig. 1(c), which show details of the topography and lateral force variations across the feature in question. These deviations are presumably induced by a complex, low-symmetry defect. Smaller deviations indicated by arrows, which may result from anisotropic defect-induced strains, are also found. Although some close-packed rows are significantly distorted in the vicinity of the defect, careful examination shows that none are interrupted. Thus the defect cannot be associated with a dislocation line crossing the surface. The marked dip in the topography and the significant variations in the spacings between successive minima strongly suggest that the defect involves at least one missing ion close to the exposed surface. No further identification appears possible, however. Atomic-scale contact mode images of crystal surfaces typically show a periodic lattice, sometimes locally distorted, but without evident point defects. This suggests that the atomic contrast in contact mode originates from a convolution of the tip and surface structure, which usually reflects the periodicity of the surface but seldom "true atomic resolution" of defects.[16] Only a few experimental studies have demonstrated that such resolution is possible[17–20] provided the contact is small and stable enough. Thus, we can assume that in the present measurements, the tip apex was indeed sharp with only a few atoms involved in the contact.

B. Friction modulation

Figure 2(a) shows representative lateral force images recorded on a defect-free area of the KBr double layer using a slow distance control setting. The average normal force was −0.01 nN in the upper half and −0.32 nN (close to the cantilever jump off force of about −0.37 nN) in the lower half. The corresponding lateral force traces along the indicated lines are plotted in Figs. 2(c) and 2(d). In Fig. 2(d), apart from noise, the tip smoothly follows the atomic corrugation of the surface lattice, resulting in a nearly perfect match between forward and backward scans, i.e., almost zero friction. In contrast, the lateral force trace in Fig. 2(c) shows a superimposed long-range modulation which reveals a strong variation of the maximum lateral force associated with the superstructure. Because the horizontal scan direction was slightly off the [001] axis of the surface, only the first seven oscillations are positioned on a line of maximal modulation of the lateral force and are considered for further analysis. A detailed view of this part in the forward direction is given in

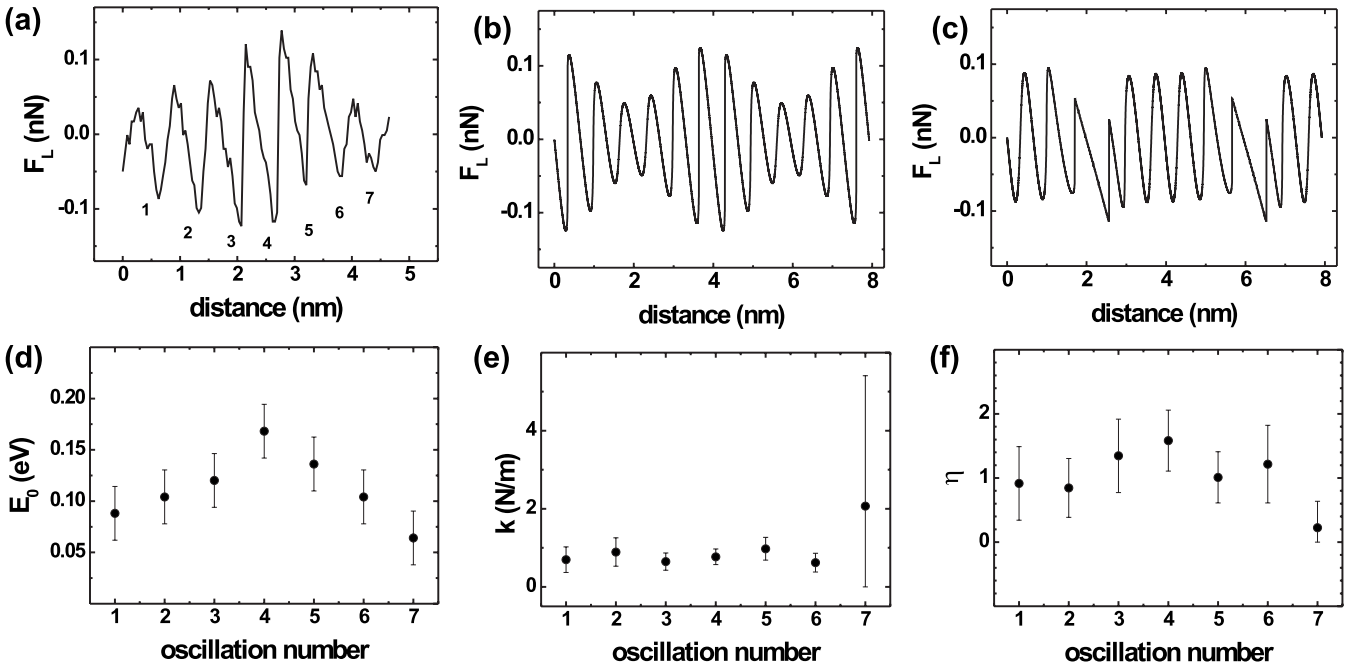

FIG. 3. (a) Forward lateral force trace along a line of maximal modulation from Fig. 2(a) (top). The gradual change from a nearly symmetric shape to a sawtooth shape indicates a transition in atomic-scale friction from smooth sliding to stick slip. (b) Simulated lateral force trace assuming a modulated energy corrugation with period $6a$ but constant stiffness in a one-dimensional Tomlinson model (Ref. 21). (c) Simulated lateral force trace assuming a modulated stiffness with period $6a$ but constant energy corrugation. (d) Corrugation amplitude E_0, (e) effective stiffness k, and (f) dimensionless parameter η determined for every oscillation within the supercell on the KBr-terminated superstructure. The transition from stick slip to smooth sliding is consistent with the change in η from values below one to values larger than one. The effective stiffness k was found to be nearly constant. The error bar for the last value of k is large because the corresponding value of η is low.

Fig. 3(a). The lateral force variation across the diagonal of the superstructure reveals a transition from a nearly sinusoidal to an asymmetric sawtooth-like shape. Moreover, the nearly perfect match between forward and backward scans for the traces at the edges of each supercell in Fig. 2(c) indicates a state of smooth sliding with ultralow friction. On the other hand, the hysteresis in the center of the supercell corresponds to atomic-scale stick-slip events with dissipation. Figure 2(b) shows the friction map obtained by subtracting the lateral force recorded in each backward scan from that recorded in the previous forward scan. Thus the regions which exhibit a strong contrast reveal the hysteresis associated with stick-slip motion, while in the gray regions the difference between forward and backward scans is small. This friction map clearly shows the transition between nearly smooth sliding to stick-slip motion of the tip while scanning at the average normal force of −0.01 nN. This value implies a near compensation between short-range repulsive and longer-range attractive forces. The net friction forces in the stick-slip range are still quite small, typically less than 20 pN. On the other hand, smooth sliding with nearly zero friction without any apparent superstructure modulation is observed close to jump off, i.e., when the short-range repulsion is minimal.

To elucidate the origin of the apparently strong modulation induced by the superstructure in the former case, we attempt to adapt the theory which has successfully described several aspects of atomic-scale friction, the transition from stick slip to smooth sliding in particular.[2] In the most simple one-dimensional version of the mechanical model proposed by Tomlinson,[21] a spring attached to a support moving at constant velocity drags an asperity over a sinusoidal surface potential. This leads to a combined surface-tip potential of the following form:

$$V = -\frac{E_0}{2}\cos\left(\frac{2\pi x_{\text{tip}}}{a}\right) + \frac{1}{2}k(x_{\text{tip}} - vt)^2, \tag{1}$$

where the effective compliance $1/k$ is the sum of the compliances of the cantilever, the tip, and the sample in contact, v is the scan velocity, and a is the lattice constant of the surface lattice.[22] The amplitude of the potential corrugation E_0 is proportional to the maximum lateral force $F_L^{\max}$,

$$E_0 = \frac{a}{\pi}F_L^{\max}. \tag{2}$$

The ratio between the curvature of the potential and the effective stiffness k is defined by the parameter η,

$$\eta = \frac{2\pi^2 E_0}{ka^2}, \tag{3}$$

where k itself can be determined from the experimentally determined slope k_{exp} of the stick stage according to[2]

$$k = \frac{\eta + 1}{\eta}k_{\text{exp}}. \tag{4}$$

Because the modulation is rather long ranged, Eqs. (2)–(4) can be used to extract approximate local values of the parameters E_0, k, η from the experimental data by applying them to successive oscillations of the lateral force. Figures 3(d)–3(f) display the parameters determined in this fashion from Fig. 3(a) with error bars estimated from 20 similar scan segments. The lattice spacing of $a=0.66$ nm of bulk KBr was used throughout because away from defects the experimental images reveal no significant variations of the surface lattice spacing. $F_L^{\max}$ was determined as the mean of the minimum (negative) lateral force $F_L=k(x-vt)$ in the forward scan and the corresponding maximum in the backward scan.

The modulation of the lateral force signal and hence $F_L^{\max}$ in Fig. 3(a) implies a strong variation of the potential corrugation E_0 between 0.06 and 0.17 eV. The slope $k_{\exp}$ varies between 0.26 and 0.56 N/m. However, Fig. 3(e) shows that the effective spring constant k does not change significantly. The variation in the slope $k_{\exp}$ is mainly associated with the correction factor in Eq. (4). The parameter η is found to vary between 0.25 and 1.5 [Fig. 3(f)]. For values of $\eta<1$ smooth sliding is expected, whereas $\eta>1$ would be stick-slip behavior. [2,3] This is consistent with the observed transition from an ultralow friction state to a stick-slip regime in the center of the supercell. The potential corrugation E_0 varies around a mean value $\overline{E_0}=0.114$ eV with the periodicity $b=6a$ of the superstructure. We therefore attempt to reproduce the experimental trace by replacing the constant E_0 in the Tomlinson model[21] by

$$\overline{E_0}\left[\alpha\cos\left(\frac{2\pi x_{\text{tip}}}{b}\right)+1\right], \tag{5}$$

where the constant $\alpha=0.45$ defines a normalized modulation amplitude.

Results of simulations which locate the minimum of the total potential closest to the previous tip position, then the next minimum when the former one disappears as the position vt of the cantilever is incremented, are shown in Figs. 3(b) and 3(c). In Fig. 3(b) a modulated energy corrugation with period $6a$ but constant stiffness of $k=1$ N/m was assumed. The long-ranged modulation as well as the transition from a nearly sinusoidal to a sawtooth shape is in good agreement with the experimental trace in Fig. 3(a). Figure 3(c) demonstrates that a cosine modulation of the local stiffness between $k=0.25$ and 1.75 N/m with a constant potential corrugation ($E_0=0.114$ eV) fails to reproduce the observed smooth modulation in the lateral force. The simulations confirm that a modulation of the potential corrugation, rather than of the local stiffness, causes the observed variation in the lateral force across the superstructure.

IV. DISCUSSION

The structure of KBr films on NaCl(100) was previously investigated by Baker and Lindgard.[12] Their Monte Carlo simulations showed that the seven to six lattice spacing mismatch caused an alignment of Cl^- and Br^- ions perpendicular to the interface at the center of each supercell; this in turn induces a rumpling which propagates to the surface of the film. Moreover, by representing the topographic corrugation of the top layer by a *sum* of cosine functions with periods a and $6a$, with amplitudes of ~0.1 Å, they could reproduce the helium diffraction intensities measured for two to six KBr layers on NaCl(100).[11] The corrugation observed in noncontact AFM measurements in the attractive range,[13] i.e., at distances several angstroms above those probed by scattered He atoms, also appears to be a sum of two contributions. However, the superstructure component is about 1 order of magnitude larger than that which fits the He diffraction data. This enhanced corrugation is likely caused by a variation of the van der Waals and electrostatic forces acting on the tip apex. Because any Fourier component with a wavelength λ along the surface decays exponentially over $\lambda/(2\pi)$ along the outward normal, the superstructure outweighs the atomic contribution at distances probed by noncontact AFM. In the present contact measurements, the disappearance of the long-ranged modulation close to cantilever jump off [see Fig. 1(b)] indicates that the modulation is enhanced when the tip is brought closer to the sample. A different mechanism must account for this behavior, as well as for the modulation (*product* rather than *sum* of two components). A possible explanation is that in the range of loads investigated here, the effective interaction area with our sharp tip is larger in the troughs of the superstructure while remaining confined within the unit cell of the superstructure. Owing to its sharpness, the tip apex induces localized compressive as well as shear deformations. Increasing the effective load leads to a larger deformation volume, which then would make the lateral force more sensitive to the interface where some ions are aligned with equally charged ones within each period of the superstructure. An additive contribution to the potential corrugation with the periodicity $b=6a$ of the superstructure, which could more readily be expected from the fit of Baker and Lindgard[12] to helium diffraction intensities, is actually present in our results. Indeed, a careful examination of Fig. 2(c) reveals that the lateral force rides on a weakly undulating baseline with the periodicity b. This trend is more evident in Fig. 1(c) away from the defect discussed previously. Being much weaker than the *a priori* unexpected modulation (product) term, this sum term was not included in our model.

As in previous atomic-scale friction measurements on NaCl and KBr(100) surfaces, the effective stiffness k is of order 1 N/m, i.e., much smaller than the lateral stiffness of the cantilever, and essentially independent of load.[2,23] This strongly suggests that k is dominated by the easy shear deformation of the tip apex.[9,24]

V. CONCLUSION

In conclusion, we have found a strong influence of the periodic interfacial mismatch on the atomic-scale friction of an ultrathin KBr film on NaCl(100). A transition from atomic-scale stick slip to smooth sliding across the unit cell of the superstructure could be attributed to a variation of the potential-energy corrugation. Numerical simulations based on a one-dimensional Tomlinson model[21] including a spatial modulation of the tip-sample interaction reproduce the measured lateral force along a line of maximal variation. These results demonstrate that the chemically homogeneous sur-

faces of such films can still exhibit significant differences in their atomic friction properties owing to small structural inhomogeneities caused by a varying local coordination of interfacial ions. The underlying mechanism merits further study. A modulation of the diffusion barriers of adsorbed species might also occur, thus suggesting possible applications of such heteroepitaxial films as templates for the self-assembly of molecules or nanoparticles on insulating substrates. Furthermore, scans across atomic-scale defects confirmed the high-resolution capabilities of friction force microscopy close to the ultralow friction state.

Note added in proof. T. Filleter *et al.*[25] recently reported contact AFM data on ultrathin KBr films grown on a Cu(100) substrate, in particular a similar but weaker modulation of the lateral force.

ACKNOWLEDGMENTS

This work was supported by the Swiss National Science Foundation and the National Center of Competence in Research on Nanoscale Science.

*Present address: Lawrence Berkeley National Laboratory, Berkeley, CA 94720, USA; sbmaier@lbl.gov

[1] C. M. Mate, G. M. McClelland, R. Erlandsson, and S. Chiang, Phys. Rev. Lett. **59**, 1942 (1987).
[2] A. Socoliuc, R. Bennewitz, E. Gnecco, and E. Meyer, Phys. Rev. Lett. **92**, 134301 (2004).
[3] S. N. Medyanik, W. K. Liu, I. H. Sung, and R. W. Carpick, Phys. Rev. Lett. **97**, 136106 (2006).
[4] M. Dienwiebel, G. S. Verhoeven, N. Pradeep, J. W. M. Frenken, J. A. Heimberg, and H. W. Zandbergen, Phys. Rev. Lett. **92**, 126101 (2004).
[5] E. Gnecco, R. Bennewitz, T. Gyalog, C. Loppacher, M. Bammerlin, E. Meyer, and H. J. Güntherodt, Phys. Rev. Lett. **84**, 1172 (2000).
[6] P. Reimann and M. Evstigneev, Phys. Rev. Lett. **93**, 230802 (2004).
[7] Y. Sang, M. Dube, and M. Grant, Phys. Rev. Lett. **87**, 174301 (2001).
[8] S. Y. Krylov, K. B. Jinesh, H. Valk, M. Dienwiebel, and J. W. M. Frenken, Phys. Rev. E **71**, 065101(R) (2005).
[9] A. Socoliuc, E. Gnecco, S. Maier, O. Pfeiffer, A. Baratoff, R. Bennewitz, and E. Meyer, Science **313**, 207 (2006).
[10] J. Park, D. Ogletree, M. Salmeron, R. Ribeiro, P. Canfield, C. Jenks, and P. Thiel, Science **309**, 1354 (2005).
[11] J. Duan, G. Bishop, E. Gillman, G. Chern, S. Safron, and J. Skofronick, Surf. Sci. **272**, 220 (1992).
[12] J. Baker and P. A. Lindgard, Phys. Rev. B **54**, R11137 (1996).
[13] S. Maier, O. Pfeiffer, T. Glatzel, E. Meyer, T. Filleter, and R. Bennewitz, Phys. Rev. B **75**, 195408 (2007).
[14] L. Howald, E. Meyer, R. Lüthi, H. Haefke, R. Overney, H. Rudin, and H.-J. Güntherodt, Appl. Phys. Lett. **63**, 117 (1993).
[15] E. Meyer, R. Overney, K. Dransfeld, and T. Gyalog, *Nanoscience: Friction and Rheology on the Nanometer Scale* (World Scientific, Singapore, 1998), pp. 351–352.
[16] F. Ohnesorge and G. Binnig, Science **260**, 1451 (1993).
[17] A. L. Shluger, R. M. Wilson, and R. T. Williams, Phys. Rev. B **49**, 4915 (1994).
[18] M. Ohta, T. Konishi, Y. Sugawara, S. Morita, M. Suzuki, and Y. Enomoto, Jpn. J. Appl. Phys., Part 1 **32**, 2980 (1993).
[19] T. Schimmel, T. Koch, J. Küppers, and M. Lux-Steiner, Appl. Phys. A: Mater. Sci. Process. **68**, 399 (1999).
[20] M. Ishikawa, S. Okita, N. Minami, and K. Miura, Surf. Sci. **445**, 488 (2000).
[21] G. Tomlinson, Philos. Mag. **7**, 905 (1929).
[22] E. Gnecco, R. Bennewitz, T. Gyalog, and E. Meyer, J. Phys. C **13**, R619 (2001).
[23] S. Maier, Y. Sang, T. Filleter, M. Grant, R. Bennewitz, E. Gnecco, and E. Meyer, Phys. Rev. B **72**, 245418 (2005).
[24] S. Y. Krylov, J. A. Dijksman, W. A. van Loo, and J. W. M. Frenken, Phys. Rev. Lett. **97**, 166103 (2006).
[25] T. Filleter, W. Paul, and R. Bennewitz, Phys. Rev. B **77**, 035430 (2008).